Introduction to Cahn-Hilliard and General Phase-Field Models

Joost de Graaf[1,*]

[1] *Institute for Theoretical Physics, Center for Extreme Matter and Emergent Phenomena, Utrecht University, Princetonplein 5, 3584 CC Utrecht, The Netherlands*

(Dated: March 4, 2026)

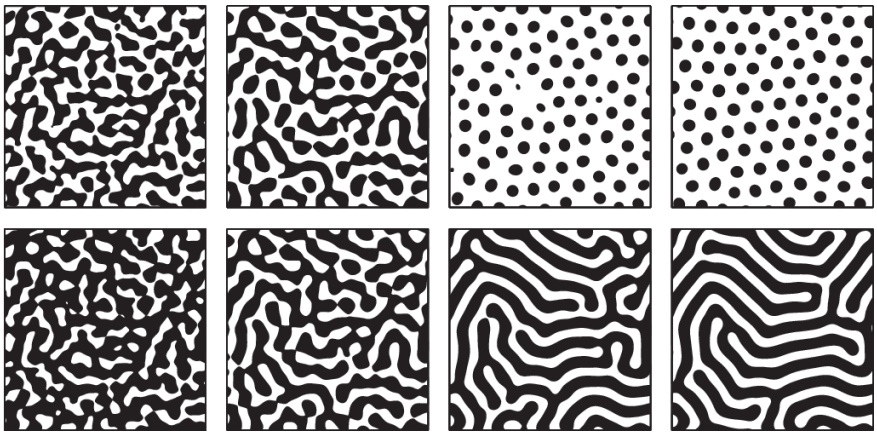

FIG. 1. **Illustration of Spinodal Decomposition:** In the above set of snapshots we see two rows of coarsening patterns that result from different initial conditions in the Cahn-Hilliard formalism. Time increases from left to right. The patterns can be understood to represent the coarse-grained evolution of particle density, or the abundance of one species of particle over another. The figure is adapted from Ref. [1].

I. INTRODUCTION

Most of the many-body physics that you have encountered in your undergraduate lectures concerns systems that are in equilibrium. Examples include the classical Ising model, site percolation, and the van-der-Waals gas[1]. For such systems, we can use the full toolset of (classical) *statistical mechanics* to understand what the properties of the system are (*i.e.*, temperature, pressure, magnetization, heat capacity, susceptibility ...). This is usually done by considering integration or summation over phase space to arrive at partition functions and free energies. Derivatives of the latter give access to the physical quantities of interest. Alternatively, one can perform renormalization-group analysis on systems near the critical point to identify the types of scaling present in the system and thereby the universality class to which it belongs. Such an analysis can also give approximative insight into the location of the continuous phase transition. Much of the characterizing power of statistical mechanics lies in the equivalence between the time-averaged and phase-space-averaged quantities for (ergodic) systems *in equilibrium*.

You will also have encountered departures from equilibrium in studying *thermodynamics*. However, recalling the efficiency of Carnot engines, you will note that the discussion is typically limited to adiabatic transients or slow-relaxation regimes, the latter of which can be handled using a near-equilibrium approximation. This situation is unsatisfying at best, as a large set of interesting

* j.degraaf@uu.nl

[1] For examples of these systems see the lecture notes for Advanced Statistical Mechanics, NS-370B, or various other textbooks on the topic, such as *Introduction to Modern Statistical Mechanics* (1987) by D. Chandler, *Statistical Mechanics, Third Edition* (2011) by P.K. Pathria and P.D. Beale, *Theory of Simple Liquids* (2006) by J.-P. Hansen and I.R. McDonald, and *Statistical Mechanics: Entropy, Order Parameters, and Complexity* (2006) by J.P. Sethna.

physical behaviors thus appear to fall outside the scope of statistical mechanics. In Soft Matter, equilibrium systems are prevalent, but equally many, if not more systems are (driven) away from equilibrium either by preparation or for a purpose. For example, some crystals that are stable in equilibrium are hard to form, as the kinetics of formation favors other structures [2–4]; the orientation and optical properties of (liquid) crystals can be finely tuned *via* (time-varying) external fields [5, 6]; and the interaction of macromolecules flowing through a thin pore can be used to determine their properties *via* current measurements [7–10].

Examples of specific relevance to the discussion in this lecture are the nucleation and growth of a dense phase from a supersaturated fluid medium, which can be used to synthesize colloidal particles [11] and the self-assembly of prefabricated colloids into crystalline structures [12, 13]. Similarly, intricate intercalating structures can form in suspended particle systems that spinodally decompose. When arrested, these can form colloidal gels [14–16], which see widespread use of in industrial, medical, and academic settings; examples include care products, printing inks, foodstuffs, crop protection, and pharmaceutical suspension formulations [17–20]. Obtaining desirable microstructures requires understanding of the coarsening dynamics in such systems. Two examples of such a process are illustrated in Fig. 1.

We will first (re)introduce a general formalism for non-equilibrium dynamics, *Dynamic Density Functional Theory* (DDFT), extending the classical density functional theory (DFT) that you have been exposed to previously. Next, we will apply this to a specific out-of-equilibrium situation, where the system starts from a homogeneous phase and coarsens. This allows us to cast DDFT into a phase-field form, deriving the *phase-field crystal model*. This can be used to study nucleation and growth of a crystal structure. We will reference an example of this and see a numerical result for dendritic growth in one of the exercises.

Inspired by the phase-field crystal model, we finally turn to the Cahn-Hilliard formalism, a simpler variant, which provides a description of spinodal decomposition. The *Cahn-Hilliard equation* — named after John W. Cahn and John E. Hilliard — traces its origin to metallurgy, for which there was an interest in predicting the microstructure of binary alloys [21]. A spinodal-decomposition derived microstructure, see Fig. 1, can impact the physical properties of the bulk material[2], when frozen in through rapid cooling, often referred to as a thermal quench. Other forms of quenching, such as exerting mechanical vibrations that are suddenly stopped, are encountered in the preparation of colloidal gels. Because the forming (and possibly arrested) system is not in equilibrium, the path by which it forms governs the physical properties at a given time. Analysing and (numerically) solving the Cahn-Hilliard equations, and equally the phase-field crystal model or DDFT, can provide insight into the microstructure underlying these properties.

Presently, it is recognized that the Cahn–Hilliard equation is applicable to a broad range of pattern-forming processes that have qualitative features of phase separation. For example, it has been applied to characterize the structure of diblock copolymers [23], model tumor growth [24], study moving contact line dynamics [25], model the distribution of plants in arid areas [26], and even to model self-propelled patterns [27]. The phase-field crystal approach bridges this scale and the particle scale, *i.e.*, what is more commonly considered the domain of particle-based simulations [28]. It is also amenable to very efficient numerical solving, as we will see, which has led to it to gain popularity in some fields. Lastly, DDFT has the most accurate dynamics and widest range of applicability [29]. However, this may be a limiting factor in studying the large-scale dynamics in the system. We refer the interested reader to the following sources to gain additional insight: [29–33]. The remainder of this text follows the discussion in Refs. [34, 35] and the lecture notes by Tristan Ursell on *Phase Separation in a Diffuse System*.

[2] As a historical curiosity, we should point out the following. It was recognized in the mid-1990s that Damascene swords — forged using Wootz steel that was first discovered in south India around the first century A.D. — utilize this type of metallurgy to achieve their high durability [22]. As this variant of sword making involves physics, it is *per definition* superior to other forms of sword manufacture, *e.g.*, involving the repeated folding of metals to achieve a similar effect, as was commonplace in Japan.

II. DENSITY FUNCTIONAL THEORY

In a previous lecture, you have seen the development of DFT. This was predicated on *Legendre transforms* between the grand potential $\Omega(\mu, V, T)$ and the canonical free energy $F(N, V, T)$, with V the volume, T the temperature, N the number of particles, and μ the chemical potential. The former is minimized with respect to the number of particles N, while the latter is minimized with respect to the chemical potential μ. From the calculations shown to you before, a density-functional form of the free energy $\mathcal{F}[\rho]$ can be recovered

$$\mathcal{F}[\rho] = \mathcal{F}_{\mathrm{id}}[\rho] + \mathcal{F}_{\mathrm{ex}}[\rho] + \int \mathrm{d}\boldsymbol{r}\, V_{\mathrm{ext}}(\boldsymbol{r})\rho(\boldsymbol{r}). \tag{1}$$

where $\rho(\boldsymbol{r})$ is the density and $V_{\mathrm{ext}}(\boldsymbol{r})$ the external potential. The term

$$\mathcal{F}_{\mathrm{id}}[\rho] = k_{\mathrm{B}}T \int \mathrm{d}\boldsymbol{r}\, \rho(\boldsymbol{r}) \left(\log\left(\rho(\boldsymbol{r})\Lambda^3\right) - 1 \right), \tag{2}$$

represents an ideal gas contribution, while $\mathcal{F}_{\mathrm{ex}}[\rho]$ encodes all intrinsic departures from ideality. Here, k_{B} is the Boltzmann constant, 'log' denotes the natural logarithm, and Λ represents the de Broglie wavelength.

In general, it is not entirely trivial to come up with good $\mathcal{F}_{\mathrm{ex}}$, as was also discussed previously. A version of $\mathcal{F}$ can be obtained from the free energy of the bulk system by making the *local-density approximation* (LDA) to obtain a functional

$$\mathcal{F}_{\mathrm{LDA}}[\rho] = \int \mathrm{d}\boldsymbol{r}\, f_{\mathrm{b}}(\rho(\boldsymbol{r})), \tag{3}$$

where we introduced

$$f_{\mathrm{b}}(\rho(\boldsymbol{r})) = \frac{F_{\mathrm{b}}(N, V, T)}{V}, \tag{4}$$

with F_{b} the bulk free energy. LDA ignores gradients in the system, the presence of which typically cause the system to incur a free-energy penalty. An approximative free energy correction is to add a square gradient (SG) term to introduce the presence of an interface

$$\mathcal{F}_{\mathrm{LDA+SG}}[\rho] = \int \mathrm{d}\boldsymbol{r} \left(f_{\mathrm{b}}(\rho(\boldsymbol{r}), T) + \frac{\kappa}{2}|\boldsymbol{\nabla}\rho(\boldsymbol{r})|^2 \right), \tag{5}$$

where κ is a prefactor that governs the width of the fluid interface, $\boldsymbol{\nabla}$ denotes the gradient operator, and $|\cdots|$ the vector norm. The term is squared, as there should not be a preferred direction in crossing the interface. When adding terms that are gradients of the density, the functional derivative of the free energy (function), takes the form

$$\left(\frac{\delta}{\delta\rho(\boldsymbol{r})} - \boldsymbol{\nabla} \cdot \frac{\delta}{\delta\boldsymbol{\nabla}\rho(\boldsymbol{r})} \right) \mathcal{F}[\rho(\boldsymbol{r})] + V_{\mathrm{ext}}(\boldsymbol{r}) - \mu = 0, \tag{6}$$

where '$\cdot$' denotes the inner product.

III. DYNAMIC DENSITY FUNCTIONAL THEORY

Several approaches were historically considered that build upon the success of 'static' DFT, so that dynamics in heterogeneous systems could also be analyzed within the DFT framework. We refer the interested reader to Ref. [30] and papers referenced therein. The starting point for the development of Dynamic Density Functional Theory, abbreviated DDFT, is the *Smoluchowski equation* [36]. A full derivation of this formalism goes beyond the scope of these lectures, but the physical intuition will be explored in the following and Exercise 1.

A. The Smoluchowski Equation

Consider a system of N Brownian particles — colloids or macromolecules suspended in a fluid medium — that are subjected to a *test* or *fictitious* external force $\boldsymbol{F}$ that derives from a potential Ψ. The external force on the j-th particle now reads $\boldsymbol{F}_j = -\boldsymbol{\nabla}_{\boldsymbol{r}_j}\Psi(\boldsymbol{r}^N)$, where $\boldsymbol{r}^N$ is the set of particle positions $\{\boldsymbol{r}_1, \ldots, \boldsymbol{r}_N\}$. The use of the subscript in the gradient indicates to which particle coordinate the derivatives are taken. In equilibrium, we know that the canonical probability density function for all N particles is given by

$$P(\boldsymbol{r}^N) = \frac{1}{Z}\exp\left[-\beta\Psi(\boldsymbol{r}^N) - \beta U(\boldsymbol{r}^N)\right]. \tag{7}$$

Here, $\beta = 1/(k_\mathrm{B}T)$, $U(\boldsymbol{r}^N)$ is the potential energy in the system that includes already present external potentials and particle interactions, and Z is a normalization factor related to the partition function. Making both P and U dependent on time and using Ψ to express forces in terms of probability, see Exercise 1, leads to the Smoluchowski equation

$$\frac{\partial}{\partial t}P(\boldsymbol{r}^N, t) = \Gamma\sum_{i=1}^{N}\boldsymbol{\nabla}_{\boldsymbol{r}_i}\cdot\left(\left[k_\mathrm{B}T\boldsymbol{\nabla}_{\boldsymbol{r}_i} + \boldsymbol{\nabla}_{\boldsymbol{r}_i}U(\boldsymbol{r}^N, t)\right]P(\boldsymbol{r}^N, t)\right). \tag{8}$$

Here, Γ is the hydrodynamic friction experienced by the particles. The above expression can be interpreted as a probability conservation equation, which is based on a flux driven by (i) diffusive spreading of $P(\boldsymbol{r}^N, t)$ with diffusion coefficient, $(k_\mathrm{B}T)\Gamma$, and (ii) a tendency of particles to move along in gradients of the potential.

Exercise 1: In this exercise we will obtain the Smoluchowski equation. The first step is to convert particle coordinates to probability densities and then through a series of physical arguments arrive at the probability conservation equation. The goal of this exercise is not to fully formalize the calculation, rather it is to gain physical intuition.

(a) Take the gradient of Eq. (7) to obtain an expression for the fictitious force exerted by the external test field in terms of the equilibrium density function P. You should arrive at $\boldsymbol{F}_j = \boldsymbol{\nabla}_{\boldsymbol{r}_j}U(\boldsymbol{r}^N) + k_\mathrm{B}T\boldsymbol{\nabla}_{\boldsymbol{r}_j}\log P(\boldsymbol{r}^N)$. Provide a physical interpretation for this expression and explain what the purpose of introducing the test field is. Hint: the notation is suggestive.

We assume slow variation of the external forcing with respect to the Brownian time τ_B. Examining dynamics on time scales longer than τ_B, it is reasonable to write

$$\boldsymbol{v}_i = -\sum_{j=1}^{N}\underline{\boldsymbol{\Gamma}}_{ij}\boldsymbol{F}_j \tag{9}$$

for the velocity of the i-th particle. Here, $\underline{\boldsymbol{\Gamma}}_{ij}$ is a mobility tensor that depends on all particle coordinates $\boldsymbol{r}^N$ at that instant in time.

(b) Why is Eq. (9) reasonable? That is, what is the underlying physical assumption for this equation to describe the dynamics of the colloids well? Hint: think back to your class on hydrodynamics for soft matter.

(c) Assume that $P(\boldsymbol{r}^N)$ and $U(\boldsymbol{r}^N)$ can be made time dependent — $P(\boldsymbol{r}^N, t)$ and $U(\boldsymbol{r}^N, t)$ — and that the expression from (a) still holds in the time-dependent form. What do you physically assume to hold in this case? Is this assumption reasonable for colloids? Hint: U is present in the equation, what is missing in terms of a Hamiltonian?

(d) Write down the continuity equation for $P(\boldsymbol{r}^N, t)$, given that the particle number is conserved and the i-th *probability* flux follows from the associated velocity $\boldsymbol{v}_i$. That is, probability is advected by the flow of particles.

Neglecting hydrodynamic interactions and assuming spherical colloids implies that we can use the mean-field expression $\underline{\boldsymbol{\Gamma}}_{ij} = \Gamma\delta_{ij}$.

(e) Show that can recover Eq. (8) from (a), Eq. (9), and (d).

Note that the Smoluchowski is thus a generalized diffusion equation. More formally, Eq. (8), can also be derived as the Fokker-Planck equation for a system of N Brownian particles in the high-friction limit [37]. We refer to a course on stochastic processes for more information.

B. Evolution of the One-Body Density

We can now use the Smoluchowski equation to derive the time evolution of the one-body density $\rho(\boldsymbol{r}, t)$, as defined by

$$\rho(\boldsymbol{r}_1, t) = N \left(\prod_{j=2}^{N} \int \mathrm{d}\boldsymbol{r}_j \right) P(\boldsymbol{r}^N, t). \tag{10}$$

The general (n-body) form of this expression reads

$$\rho(\boldsymbol{r}^n, t) = \frac{N!}{(N-n)!} \left(\prod_{j=n+1}^{N} \int \mathrm{d}\boldsymbol{r}_j \right) P(\boldsymbol{r}^N, t), \tag{11}$$

where $\boldsymbol{r}^n$ is a set containing $n < N$ particle coordinates and the prefactor accounts for combinatorics and normalization. If we also assume that all interactions in the system are given by pair potentials $v_2(\boldsymbol{r}_i, \boldsymbol{r}_j)$, we can write

$$U(\boldsymbol{r}^N, t) = \sum_{i=1}^{N} V_{\mathrm{ext}}(\boldsymbol{r}_i, t) + \frac{1}{2} \sum_{i=1}^{N} \sum_{j \neq i} v_2(\boldsymbol{r}_i, \boldsymbol{r}_j). \tag{12}$$

Subsequently integrating Eq. (8) using this expression, we obtain the expression for the time evolution of $\rho(\boldsymbol{r}, t)$

$$\begin{aligned} \Gamma^{-1} \frac{\partial \rho(\boldsymbol{r}_1, t)}{\partial t} &= k_{\mathrm{B}} T \nabla^2_{\boldsymbol{r}_1} \rho(\boldsymbol{r}_1, t) + \boldsymbol{\nabla}_{\boldsymbol{r}_1} \cdot \left[\rho(\boldsymbol{r}_1, t) \boldsymbol{\nabla}_{\boldsymbol{r}_1} V_{\mathrm{ext}}(\boldsymbol{r}_1, t) \right] \\ &\quad + \boldsymbol{\nabla}_{\boldsymbol{r}_1} \cdot \int \mathrm{d}\boldsymbol{r}_2 \, \rho(\boldsymbol{r}_1, \boldsymbol{r}_2, t) \boldsymbol{\nabla}_{\boldsymbol{r}_1} v_2(\boldsymbol{r}_1, \boldsymbol{r}_2). \end{aligned} \tag{13}$$

Here, we have introduced the two-body density $\rho(\boldsymbol{r}_1, \boldsymbol{r}_2, t)$. You might recognize elements of the hierarchy of equations in this expression that you obtain when you consider the evolution of density fields that follow from the Liouville equation for many-body Hamiltonian dynamics.

Exercise 2: Perform the somewhat tedious partial integrations required to arrive at Eq. (13). While this exercise may be instructive, it is probably better to ignore it until the very end of your problem class / self-allotted homework time.

We proceed by analyzing the interaction term and introducing the *direct correlation function*

$$c(\boldsymbol{r}) = -\frac{1}{k_{\mathrm{B}}T}\frac{\delta\mathcal{F}_{\mathrm{ex}}[\rho]}{\delta\rho(\boldsymbol{r})}, \tag{14}$$

which measures the correlation between two particles that is *not* mediated by the presence of other particles in the solvent. The expression in Eq. (14) is the first element is a series of correlation functions that are obtained by taking higher-order functional derivatives of the excess free energy. In dilute gases, $c(\boldsymbol{r})$ simply specifies the pair-wise interaction between particles. In denser systems, $c(\boldsymbol{r})$ plays the role of an effective mean-field for the particle interactions. This can be understood by introducing the expression for the ideal and excess free-energy functional, and rewriting

$$k_{\mathrm{B}}T\log(\Lambda^3\rho(\boldsymbol{r})) + \frac{\delta\mathcal{F}_{\mathrm{ex}}[\rho]}{\delta\rho(\boldsymbol{r})} + V_{\mathrm{ext}}(\boldsymbol{r}) - \mu = 0; \tag{15}$$

$$\Rightarrow \quad \rho(\boldsymbol{r}) = \rho_{\mathrm{bulk}}\exp\left(-\beta V_{\mathrm{ext}}(\boldsymbol{r}) + c(\boldsymbol{r}) + \beta\mu\right). \tag{16}$$

Here, we have introduced the bulk density ρ_{bulk} and slightly abused the notation to remove the equilibrium '0' subscript. From Eq. (16) it becomes clear that $c(\boldsymbol{r})$ modulates the spatial density *via* the interaction term. Note that we must have $\lim_{|\boldsymbol{r}|\to\infty} c(\boldsymbol{r}) = -\beta\mu$. Thus, we have a self-consistent equation for $\rho(\boldsymbol{r})$, as $c(\boldsymbol{r})$ depends on the density profile itself.

In equilibrium, for a system where particles interact solely by pair potentials, the gradient of the one-body direct correlation function $c(\boldsymbol{r})$ is related to the two-body density *via*

$$-k_{\mathrm{B}}T\rho(\boldsymbol{r})\boldsymbol{\nabla}_{\boldsymbol{r}}c(\boldsymbol{r}) = \int \mathrm{d}\boldsymbol{r}'\,\rho(\boldsymbol{r},\boldsymbol{r}',t)\boldsymbol{\nabla}_{\boldsymbol{r}}v_2(\boldsymbol{r},\boldsymbol{r}'). \tag{17}$$

This follows straightforwardly from the technical manipulations you performed in Exercise 2 and the definition of $c(\boldsymbol{r})$.

C. Expressions for Dynamic Density Functional Theory

We now make the approximation that the direct-correlation-function identities also hold out of equilibrium, such that we arrive at the DDFT equation

$$\Gamma^{-1}\frac{\partial\rho(\boldsymbol{r},t)}{\partial t} = \boldsymbol{\nabla}\cdot\left[\rho(\boldsymbol{r},t)\boldsymbol{\nabla}\frac{\delta\mathcal{F}[\rho(\boldsymbol{r},t)]}{\delta\rho(\boldsymbol{r},t)}\right], \tag{18}$$

where we have

$$\mathcal{F}[\rho(\boldsymbol{r},t)] = k_{\mathrm{B}}T\int \mathrm{d}\boldsymbol{r}\,\rho(\boldsymbol{r},t)\left(\log\left(\rho(\boldsymbol{r},t)\Lambda^3\right) - 1\right) + \mathcal{F}_{\mathrm{ex}}[\rho(\boldsymbol{r},t)] + \int \mathrm{d}\boldsymbol{r}\,V_{\mathrm{ext}}(\boldsymbol{r},t)\rho(\boldsymbol{r},t). \tag{19}$$

The first term is a time-dependent variant of the ideal-gas expression of Eq. (2), the second part takes into account the non-idealities in the particle interactions, and the third introduces a time-dependent potential working on the system.

Exercise 3: Use Eq. (18) to obtain the diffusion equation for an ideal Brownian gas, *i.e.*, a colloidal gas for which there are no particle interactions.

D. Further Considerations for DDFT

The concept of a chemical potential is applicable out of equilibrium, and we may therefore rewrite Eq. (18) as follows

$$\Gamma^{-1}\frac{\partial\rho(\boldsymbol{r},t)}{\partial t} = \boldsymbol{\nabla}\cdot\left[\rho(\boldsymbol{r},t)\boldsymbol{\nabla}\mu(\boldsymbol{r},t)\right], \tag{20}$$

where the chemical potential now depends on position and time. We can take the perspective that $\Gamma\rho(\boldsymbol{r},t)$ is density-dependent mobility for the particle, with the (negative) gradient of the chemical potential acting as a thermodynamic driving force for the evolution of the particle density. Note that this expression for the mobility is not particularly realistic, since the mobility of individual particles suspended in a fluid is highly dependent on local density in a non-linear fashion [38]. However, we had already eliminated a more accurate description at the level of the Smoluchowski approximation. If one would want a better DDFT in this regard, that is the place to start.

The expression in Eq. (20) can be used even when the local chemical potential is not integrable to a free-energy functional[3]. It is good to note that, in equilibrium, we regain the expected behavior. This suggests that, provided V_{ext} does not depend on time, the result of DDFT reduces to that of DFT for a given system, irrespective of initial condition, *i.e.*, $\lim_{t\to\infty}\rho(\boldsymbol{r},t) = \rho_0(\boldsymbol{r})$. Lastly, we should note that stochastic variants of DDFT also exist, the above introduction provides only the deterministic variant. We refer an interested reader to Ref. [29] for an overview.

IV. PHASE-FIELD CRYSTAL METHOD FROM DDFT

In the following, we will assume that $V_{\text{ext}}(\boldsymbol{r},t) = 0$ and that we have an initially (almost) homogenous fluid. We will chart the evolution of the fluctuations in density $\tilde{\rho}(\boldsymbol{r},t) = \rho(\boldsymbol{r},t) - \rho_{\text{h}}$ about the homogeneous bulk density ρ_{h}. The final goal is to study a system that spinodally decomposes and chart the initial departures away from the homogeneous fluid (possibly after a quench into the spinodal region). Two phases must form, which implies a free-energy functional that has an ideal and excess part

$$\mathcal{F}_{\text{sd}}[\rho(\boldsymbol{r},t)] = k_{\text{B}}T\int \mathrm{d}\boldsymbol{r}\,\rho(\boldsymbol{r},t)\left(\log\left(\rho(\boldsymbol{r},t)\Lambda^3\right) - 1\right) + \mathcal{F}_{\text{ex}}[\rho(\boldsymbol{r},t)], \tag{21}$$

where $\mathcal{F}_{\text{ex}}[\rho(\boldsymbol{r},t)]$ leads to phase separation through interactions.

Exercise 4: When you insert Eq. (21) into Eq. (18), this gives

$$(\Gamma k_{\text{B}}T)^{-1}\frac{\partial\tilde{\rho}(\boldsymbol{r},t)}{\partial t} = \nabla^2\tilde{\rho}(\boldsymbol{r},t) - \rho_{\text{h}}\nabla^2 c(\boldsymbol{r},t) - \boldsymbol{\nabla}\cdot\left[\tilde{\rho}(\boldsymbol{r},t)\boldsymbol{\nabla}c(\boldsymbol{r},t)\right], \tag{22}$$

where ∇^2 is the Laplacian and we have reintroduced the dynamic one-body direct correlation function $c(\boldsymbol{r},t)$. Use properties of the Helmholtz free-energy functional and the one-body direct correlation function to arrive at Eq. (22). A potential route toward studying spinodal decomposition is to analyze the derivatives of $c(\boldsymbol{r},t)$ and express these in terms of the two-body correlation function [34]. We will follow a different route in these notes.

The next step in approaching phase separation is to expand both $\mathcal{F}_{\text{id}}$ and $\mathcal{F}_{\text{ex}}$ appropriately in terms of $\tilde{\rho}(\boldsymbol{r},t)$. As Cahn-Hilliard is an effective *phase-field* theory, we introduce a notation that

[3] Terms that break integrability of the chemical potential have been explored to gain understanding of (strongly) non-equilibrium physics and coexistence in active matter [39].

will eventually lead to this formalism[4] $\phi(\boldsymbol{r},t) = \tilde{\rho}(\boldsymbol{r},t)/\rho_\mathrm{h}$. Assuming that the departure away from ρ_h can be captured by a Taylor approximation, we arrive at the following expression for the ideal free-energy functional

$$\begin{aligned}\mathcal{F}_\mathrm{id}[\phi] = F_\mathrm{id}(\rho_\mathrm{h}) + k_\mathrm{B}T\left[\rho_\mathrm{h}\log(\Lambda^3\rho_\mathrm{h})\right]\int \mathrm{d}\boldsymbol{r}\,\phi(\boldsymbol{r},t) \\ + k_\mathrm{B}T\rho_\mathrm{h}\int \mathrm{d}\boldsymbol{r}\left[\frac{1}{2}\phi^2(\boldsymbol{r},t) - \frac{1}{6}\phi^3(\boldsymbol{r},t) + \frac{1}{12}\phi^4(\boldsymbol{r},t) - \cdots\right].\end{aligned} \tag{23}$$

The term $F_\mathrm{id}(\rho_\mathrm{h})$ is an irrelevant constant that gives the bulk free-energy contribution in the homogenous phase with density ρ_h.

Exercise 5: Perform the expansion required to obtain Eq. (23). What do the terms contribute to the dynamics of the field and why?

The excess free-energy functional is usually approximated as

$$\mathcal{F}_\mathrm{ex}[\phi] = F_\mathrm{ex}[\rho_h] - \frac{k_\mathrm{B}T}{2}\rho_\mathrm{h}^2\int \mathrm{d}\boldsymbol{r}\,\phi(\boldsymbol{r},t)\left(c_0 - c_2\nabla^2 + c_4\nabla^4 - \cdots\right)\phi(\boldsymbol{r},t), \tag{24}$$

using an expansion of the Fourier transform of the two-particle direct correlation function [35]. Here, the c_i ($i \in \{0,2,4\}$) are constants resulting from the expansion. These prefactors can also be associated with features of the solid phase, such as elasticity. The bulk term $F_\mathrm{ex}(\rho_\mathrm{h})$ is an irrelevant constant factor to our derivation.

Let us now go through the major steps in this expansion. Consider small-density deviations $\delta\rho(\boldsymbol{r}) = \rho(\boldsymbol{r}) - \rho_h$ about a uniform, homogenous state. To quadratic order, we then have that

$$\beta\Delta\mathcal{F}_\mathrm{ex} = -\frac{1}{2}\int \frac{\mathrm{d}\boldsymbol{k}}{(2\pi)^3}\hat{c}^{(2)}(k;\rho_0)|\delta\hat{\rho}(k)|^2 + \cdots, \tag{25}$$

where $\hat{c}^{(2)}(k)$ is the 3D Fourier transform of $c^{(2)}(r)$:

$$\hat{c}^{(2)}(k) = 4\pi\int_0^\infty \mathrm{d}r\, r^2 c^{(2)}(r)\frac{\sin(kr)}{kr} \tag{26}$$

and the real-space two-body direct correlation function follows from the functional derivative

$$c^{(2)}(\boldsymbol{r},\boldsymbol{r}') = -\beta\frac{\delta^2\mathcal{F}_\mathrm{ex}[\rho]}{\delta\rho(\boldsymbol{r})\delta\rho(\boldsymbol{r}')}. \tag{27}$$

Note that we have further assumed an interaction that depends only on the separation $|\boldsymbol{r}-\boldsymbol{r}'|$.

Exercise 6: Perform the expansion and justify why the first-order term drops out.

For slowly varying fields, we can expand the Fourier transform of the two-body direct correlation function around $k = 0$ to obtain

$$\hat{c}^{(2)}(k) = \hat{C}_0 + \hat{C}_2k^2 + \hat{C}_4k^4 + \mathcal{O}(k^6), \tag{28}$$

[4] You may recall that density itself is not an appropriate order parameter in a (phase-field) Landau sense, as order parameters are not thermodynamic state variables. However, (reduced) density gap, the change in density when undergoing a phase transition is an order parameter, hence we can use $\phi(\boldsymbol{r},t)$ as introduced here.

with *phase-space coefficients* (moments of $c^{(2)}$)

$$\hat{C}_0 = 4\pi \int_0^\infty \mathrm{d}r\, r^2 c^{(2)}(r), \tag{29}$$

$$\hat{C}_2 = -\frac{4\pi}{3!} \int_0^\infty \mathrm{d}r\, r^4 c^{(2)}(r), \tag{30}$$

$$\hat{C}_4 = \frac{4\pi}{5!} \int_0^\infty \mathrm{d}r\, r^6 c^{(2)}(r). \tag{31}$$

Exercise 7: Why are there no odd terms to the above expansion? Provide a physical intuition based on symmetry, justify your answer using a *few* words only.

Inserting Eq. (28) into Eq. (25) and inverse-transforming (labelling the coefficients $\hat{C}_i \to c_i$) gives the desired gradient expansion

$$\beta\Delta\mathcal{F}_{\mathrm{ex}} = -\frac{1}{2}\int \mathrm{d}\boldsymbol{r}\, \delta\rho \left[c_0 - c_2\nabla^2 + c_4\nabla^4 - \cdots\right] \delta\rho. \tag{32}$$

Upon introducing our definition of the density expansion, $\rho = \rho_h(1+\phi)$, this yields

$$\beta\Delta\mathcal{F}_{\mathrm{ex}} = -\frac{1}{2}\rho_h^2 \int \mathrm{d}\boldsymbol{r}\, \phi \left(c_0 - c_2\nabla^2 + c_4\nabla^4 - \cdots\right) \phi. \tag{33}$$

Exercise 8: Rework the terms in Eq. (33) to physically interpret c_0, and identify the square-gradient stiffness $\kappa = \frac{k_\mathrm{B}T}{2}c_2$ and the biharmonic coefficient $\lambda = -\frac{k_\mathrm{B}T}{2}c_4$. Comment on the sign of κ that is required to ensure stability. Now assume $\rho_h \downarrow 0$ and show that $c^{(2)}(r) = -\beta u(r) + \mathcal{O}(\rho_0)$ with $u(r)$ the pair potential. Rewrite c_0, c_2, and c_4 in terms of integrals over $u(r)$ and comment on the physical requirements for $u(r)$ to ensure stability.

To make the above abstract notion more explicit, let us examine a few examples. For a Gaussian repulsive potential,

$$u(r) = \epsilon e^{-r^2/\sigma^2}, \tag{34}$$

with $\epsilon > 0$ the potential strength and σ the range, we have that

$$c^{(2)}(r) \approx -\beta\epsilon e^{-r^2/\sigma^2}, \tag{35}$$

in the dilute limit. This gives the Fourier-space expression

$$\hat{c}^{(2)}(k) = -\beta\epsilon(\pi^{3/2}\sigma^3)e^{-(k\sigma/2)^2}, \tag{36}$$

for which a Taylor expansion reveals

$$c_0 = -\beta\epsilon\pi^{3/2}\sigma^3; \tag{37}$$

$$c_2 = +\beta\epsilon\pi^{3/2}\sigma^5/4; \tag{38}$$

$$c_4 = -\beta\epsilon\pi^{3/2}\sigma^7/32. \tag{39}$$

Thus, we conclude that the square gradient stiffness $\kappa > 0$ and the biharmonic coefficient $\lambda > 0$, see Exercise 8 for the definitions.

Exercise 9: Repeat this analysis for a Yukawa and hard-sphere interaction, as well as a square-well potential. What conclusions can you draw about the nature of the short-ranged interactions and the signs of the c_i?

Following this section, we conclude that *shape* of $\hat{c}^{(2)}(k)$ near $k = 0$ encodes the physics: c_0 sets the bulk quadratic curvature, c_2 the interfacial penalty $|\boldsymbol{\nabla}\phi|^2$, and c_4 the preferred mesoscale. In phase-field-crystal models, we therefore have that when C_0 changes sign a transition can occur from a homogenous to a patterned phase, while $c_2 > 0$; $C_4 > 0$ is needed for stability.

Introducing the above expansions in terms of $\phi(\boldsymbol{r}, t)$ into our DDFT, see Eq. (18), we can now come to a phase-field description of the evolution of a system. Here, we make the further reducing assumption that the mobility factor $\Gamma\rho(\boldsymbol{r}, t)$ is well approximated by $\Gamma\rho_{\mathrm{h}}$. The implication is that particle mobility is only proportional to the overall particle density of the starting phase, which was constant to begin with. Clearly, this dynamics is approximative in nature, but we know at which stages we made reducing assumptions. The resulting expression for the dynamics of the phase field is then

$$\frac{\partial\phi(\boldsymbol{r},t)}{\partial t} = D\nabla^2\left[\phi(\boldsymbol{r},t) - \frac{1}{2}\phi(\boldsymbol{r},t)^2 + \frac{1}{3}\phi(\boldsymbol{r},t)^3 - \left(\hat{c}_0 - \hat{c}_2\nabla^2 + \hat{c}_4\nabla^4 + \cdots\right)\phi(\boldsymbol{r},t)\right]. \tag{40}$$

Here, $D = k_{\mathrm{B}}T\Gamma$, denotes the diffusion coefficient of the colloidal particles. Equation (40) is known as the *phase-field crystal* model [32], which describes particles as a field and can be used to study nucleation and growth, see Fig. 2. We will numerically solve it ourselves for another set of coefficients and initial conditions in Exercise 13.

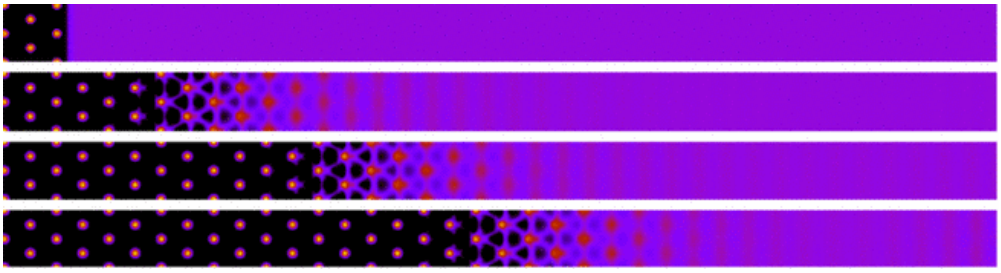

FIG. 2. **Growth in the Phase-Field Crystal Model:** Time series of the evolution of the phase field as a function of time, running from top to bottom. In this case, a crystal lattice with a linear front grows out into the fluid phase. The figure is reproduced from Ref. [35].

V. CAHN-HILLIARD FOR SPINODAL DECOMPOSITION

In examining Eq. (40) we recognize the power of writing more general phase-field expressions. The Cahn-Hilliard formalism can be seen as a simpler variant of the phase-field crystal. The original work by Cahn relied more heavily on derivation from microscopic laws [21] and is worth examining. A common perturbative expression — suited for small perturbations away from homogeneous in binary phase separation — is given by

$$\frac{\partial\phi(\boldsymbol{r},t)}{\partial t} = D\nabla^2\left[\phi(\boldsymbol{r},t)^3 - \phi(\boldsymbol{r},t) - \kappa\nabla^2\phi(\boldsymbol{r},t)\right], \tag{41}$$

where κ governs the interface width. Note that here we do not have a quadratic term in ϕ, as was the case with the phase-field crystal. This is simply because our reference point is assumed to be

the critical composition. If you have a reference point that is shifted with respect to the critical composition, you can redefine ϕ and recover a quadratic term.

Equation (41) follows from a (Landau) phase-field free-energy functional *via*

$$\frac{\partial \phi(\boldsymbol{r},t)}{\partial t} = -\boldsymbol{\nabla}\cdot\boldsymbol{j}(\boldsymbol{r},t); \tag{42}$$

$$\boldsymbol{j}(\boldsymbol{r},t) = -D\boldsymbol{\nabla}\mu(\boldsymbol{r},t); \tag{43}$$

$$\mu(\boldsymbol{r},t) = \left(\frac{\delta}{\delta\phi(\boldsymbol{r},t)} - \boldsymbol{\nabla}\cdot\frac{\delta}{\delta\boldsymbol{\nabla}\phi(\boldsymbol{r},t)}\right)\mathcal{F}[\phi(\boldsymbol{r})]; \tag{44}$$

$$\mathcal{F}[\phi(\boldsymbol{r},t)] = \int \mathrm{d}\boldsymbol{r}\left[\frac{1}{4}\left(\phi(\boldsymbol{r},t)^2-1\right)^2 + \frac{\kappa}{2}|\boldsymbol{\nabla}\phi(\boldsymbol{r},t)|^2\right], \tag{45}$$

where in Eq. (45), we recognize 4th-order Landau double-well structure in $\phi(\boldsymbol{r},t)$, which describes a system that phase separates into $\phi(\boldsymbol{r},t) = \pm 1$. This expression may also be derived from the free-energy functional for a binary mixture, for which the above Landau expression follows from Taylor expanding the entropy of mixing and interaction terms, see for example Ref. [31].

Most modern approaches dealing with Cahn-Hilliard instead use the more general form

$$\mathcal{F}[\phi(\boldsymbol{r},t)] = \int \mathrm{d}\boldsymbol{r}\left[\frac{\alpha_1}{2}\phi(\boldsymbol{r},t)^2 + \frac{\alpha_2}{4}\phi(\boldsymbol{r},t)^4 + \frac{\kappa}{2}|\boldsymbol{\nabla}\phi(\boldsymbol{r},t)|^2\right]. \tag{46}$$

Here, α_1 is a prefactor that depends on temperature, such that it changes sign near the critical point $\alpha_1 \approx \alpha(T - T_\mathrm{c})$, with T_c the critical temperature and α a Taylor expansion coefficient. The coefficient α_2 is usually chosen to be temperature independent and must be positive.

Exercise 10: Assume we are working in one dimension (1D), with coordinate z, $\alpha_1 = (1 - T/T_\mathrm{c})$, $\alpha_2 = 1/3$, and that the system is stationary.

(a) Show that you can rewrite the (*time-independent*) Cahn-Hilliard equation that follows from Eq. (46) to read

$$-\eta(\chi) + \eta(\chi)^3 - \frac{1}{2}\frac{d^2}{d\chi^2}\eta(\chi) = 0. \tag{47}$$

Here, $\eta(z) = \phi(z)/\phi_*$ with $\phi_* = \sqrt{3(T/T_\mathrm{c} - 1)}$ and $\chi = z/\xi$ with $\xi = \sqrt{6\kappa}/\phi_*$.

(b) Show that the exact solution reads $\eta(\chi) = \pm\tanh(\chi)$, when $\lim_{z\to\pm\infty}\phi(z) = \pm\phi_*$. Sketch the result and give a physical interpretation to ϕ_* and ξ.

(c) Argue how this captures the formation of an interface both in the >1D Ising model and phase separation in a binary mixture (*e.g.*, as described by Flory-Huggins theory).

Using this result you can compute the surface tension as well, but we will not do so presently. It turns out that $\eta(\chi) = \pm\tanh(\chi)$ is not the only solution to the stationary problem. There is a whole family of solutions called soliton-lattice solutions, which are interesting, but go a bit beyond the current material. They can be used to describe the coalescence of smaller domains, until the two-distinct phases 'ground state' solution given by $\tanh(\chi)$ is obtained.

A. Characterizing Spinodal Decomposition

In Exercise 10 you have already seen that the Cahn-Hilliard equation gives us two bulk phases with a different order parameter, which are separated by an interface of a width that diverges upon approaching the critical point (from below). In this last section, we will consider the scaling and features of spinodal decomposition as predicted by Cahn-Hilliard theory. This analysis relies on studying the Fourier modes of the equation, but can readily be transposed to the phase-field crystal model [35] and the DDFT [34].

As a first step we rewrite the Cahn-Hilliard equation following from the free-energy functional in Eq. (46). We introduce τ as a natural time and λ as a natural length scale. We obtain

$$\frac{\partial \phi}{\partial \tilde{t}} = \tilde{\nabla}^2 \left[-\frac{D\tau\alpha_1}{\lambda^2} \left(\frac{\alpha_2}{-\alpha_1}\phi^3 - \phi \right) - \frac{\kappa\tau D}{\lambda^4}\tilde{\nabla}^2\phi \right], \tag{48}$$

where the use of '$\sim$' indicates the new reduced units and we have introduced minus signs, as α_1 must be negative in the regime where the decomposition can take place. We have that $-\alpha_1/\alpha_2 = (\phi^*)^2$ (solving for the non-interfacial stationary ϕ), and by choosing $\tau = \kappa/(\alpha_1^2 D)$ and $\lambda^2 = -\kappa/\alpha_1$ we arrive at

$$\frac{\partial \tilde{\phi}}{\partial \tilde{t}} = \tilde{\nabla}^2 \left[\left(\tilde{\phi}^2 - 1 \right) \tilde{\phi} - \tilde{\nabla}^2 \tilde{\phi} \right], \tag{49}$$

with $\tilde{\phi} = \phi/\phi^*$. Note that this form is slightly different from the one you arrived at in Exercise 10, but it is similar in spirit.

Now we are in a position to Fourier transform Eq. (49), for which we drop the tildes to ease the notation, and analyze the growth of various modes *via* the transform

$$\phi(\boldsymbol{r}, t) = \int \mathrm{d}\boldsymbol{k}\, \check{\phi}(\boldsymbol{k}, t) e^{-i\boldsymbol{k}\cdot\boldsymbol{r}}. \tag{50}$$

In order to make this analysis a bit easier, we can assume $\tilde{\phi}$ is small and expand to linear order. The resulting Fourier-space Cahn-Hilliard dynamics is given by

$$\frac{\partial \check{\phi}}{\partial t} = \left(|\boldsymbol{k}|^2 - |\boldsymbol{k}|^4 \right) \check{\phi}, \tag{51}$$

which has the general solution

$$\check{\phi}(\boldsymbol{k}, t) = \check{\phi}(\boldsymbol{k}, 0) \exp \left[\left(|\boldsymbol{k}|^2 - |\boldsymbol{k}|^4 \right) t \right]. \tag{52}$$

It should be immediately clear that for $|\boldsymbol{k}| = 2^{-1/2}$ the growth is greatest ($|\boldsymbol{k}|^2 - |\boldsymbol{k}|^4$ is maximized), all wavelengths with $|\boldsymbol{k}| < 1$ grow exponentially, while for $|\boldsymbol{k}| > 1$ they decay exponentially.

The above analysis makes it clear that growth of a pattern is promoted when the system is quenched from a homogeneous state. However, the fact that there is fastest growth at a wave number of $|\boldsymbol{k}| = 2^{-1/2}$ not extremely insightful. Firstly, Cahn-Hilliard provides an approximative result for the very earliest times of spinodal decomposition. As you will recall, there were a number of strongly reducing assumptions by which we arrived at the phase-field crystal model. Cahn-Hilliard is approximative beyond even that model. A more thorough analysis of the evolution of perturbations can be made using DFT [34]. However, it is also commonplace to numerically chart the evolution of the phase field, for example, see Fig. 3. We refer the interested reader to

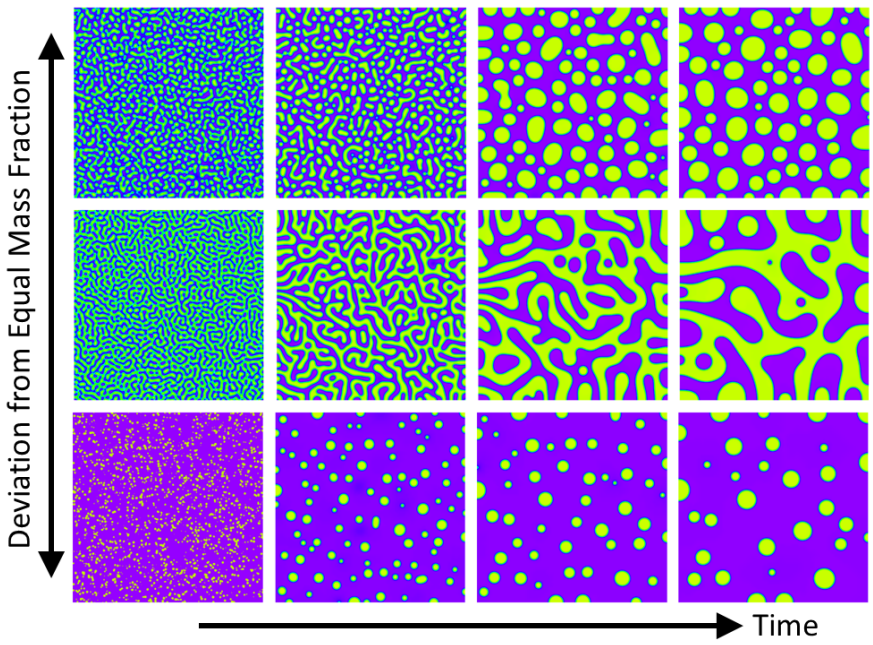

FIG. 3. **Solutions to the Cahn-Hilliard Equation:** The above set of snapshots shows three rows of coarsening patterns that result from different initial mass fractions (values of ϕ) in the Cahn-Hilliard formalism. Time increases from left to right. The figure is adapted from Ref. [40].

Refs. [40, 41] for specifics on implementing this approach.

Exercise 11: Assume we have a free-energy density of the following form

$$f(\phi, \nabla^2\phi, \nabla^4\phi) = \left(\lambda q_0^4 - a\Delta_0\right)\frac{\phi^2}{2} + u\frac{\phi^4}{4} + \lambda q_0^2\phi\nabla^2\phi + \frac{\lambda}{2}\phi\nabla^4\phi. \tag{53}$$

where λ, q_0, a, Δ_0, and u are constants that specify the properties of the system. You can assume that our result for functional derivatives, as presented in the notes, can be generalized to

$$\frac{\delta\mathcal{F}[\phi(\boldsymbol{r},t)]}{\delta\phi(\boldsymbol{r},t)} = \sum_{n=0}^{\infty}(-1)^n\nabla^n\cdot\frac{\partial f}{\partial(\nabla^n\phi)}, \tag{54}$$

where the $\cdot$ indicates an inner product when there are uneven terms.

(a) Show that the above free-energy functional gives this

$$\mu(\boldsymbol{r},t) = \left(\lambda q_0^4 - a\Delta_0\right)\phi + u\phi^3 + 2\lambda q_0^2\nabla^2\phi + \lambda\nabla^4\phi \tag{55}$$

form of the (local) chemical potential.

(b) Assuming that the ϕ field is subject to conservative dynamics and diffuses with coefficient D, derive the partial differential equation

$$\frac{\partial\phi(\boldsymbol{r},t)}{\partial t} = D\nabla^2\left[-a\Delta_0\phi + u\phi^3 + \lambda(q_0^2+\nabla^2)^2\phi\right], \tag{56}$$

for the dynamics of the ϕ field.

(c) Introducing reduced variables $\tilde{\phi} = \phi\sqrt{u/(\lambda q_0^4)}$, $\tilde{t} = tD\lambda q_0^6$, and $\tilde{\nabla} = \nabla/q_0$, allows us to write

$$\frac{\partial\tilde{\phi}}{\partial\tilde{t}} = \tilde{\nabla}^2\left[\left((1+\tilde{\nabla}^2)^2 - \epsilon\right)\tilde{\phi} + \tilde{\phi}^3\right], \tag{57}$$

provide ϵ and give a physical interpretation to this quantity.

(d) Use the Fourier transform

$$\phi(\boldsymbol{r},t) = \int \mathrm{d}\boldsymbol{k}\,\check{\phi}(\boldsymbol{k},t)e^{-i\boldsymbol{k}\cdot\boldsymbol{r}}, \tag{58}$$

and an expansion to obtain an equation for the modes of growth. What is the fastest growing mode? Which modes are conserved and why does this make physical sense?

Exercise 12: Let us now return to the Cahn-Hilliard equation, Eq. (49) and subject this to further analysis. Assume we are operating in one dimension (1D) and that we have a nearly homogenous solution $\phi = \phi_0 + \epsilon\phi_1(x,t)$. Here, ϕ_0 is the spatially and temporally constant solution that is perturbed by ϕ_1, with ϵ the expansion coefficient.

(a) Assume $\epsilon \ll 1$ and expand Eq. (49) to linear order in ϵ.

(b) Make the ansatz that $\phi_1(x,t) = \exp(ikx+\beta t)$, with k and β some constants to be determined. Determine β as a function of k.

(c) Using your above dispersion relation, and assuming that k is real, we realize that β gives the growth rate of any wave with wave number k. Solve $\beta(k) = 0$ to establish the cut-off wave number k_c.

(d) Only positive, real valued solutions for k_c make physical sense, explain why. Use this to establish bounds on ϕ_0.

(e) What is the physical interpretation of these bounds? Relate them to the properties of the reduced free energy that underlies Eq. (49).

(f) Repeat the procedure on Eq. (57). What do you learn?

Exercise 13: Consider the Cahn-Hilliard (CH) equation with a quartic local free-energy density in reduced form. Use the `Python`-style pseudocode provided on the next page, to implement a semi-implicit Fourier spectral scheme on a periodic 2-dimensional grid. Translate this into working code (NumPy + FFT) code, in order to run a spinodal decomposition from random initial data (small amplitude white noise), and analyze structure growth, *e.g.*, *via* the dominant wave number of $|\hat{\phi}(\boldsymbol{k},t)|^2$. The following will help: (i) Work with the reduced form of the equations, no need to have addional complication by having a bunch of parameters floating around. (ii) Choose dt small enough to remain stable; verify that $\langle\phi\rangle$ is conserved to numerical tolerance. (iii) Start from $\phi_0 = \phi_0^{\mathrm{mean}} + 10^{-3} \times \mathrm{uniform}[-1,1]$ with $\phi_0^{\mathrm{mean}} \in \{0, 0.2\}$. (iv) Produce and discuss snapshots of $\phi(x,y,t)$ and the time dependence of the peak wave number of the structure factor.

```
# Parameters and grid
Nx, Ny = 256, 256            # grid sizes
Lx, Ly = 1.0, 1.0            # domain lengths
dx, dy = Lx/Nx, Ly/Ny
dt = 1e-4                    # time step (choose stable value)
Tend = 2.0                   # final time

# Wavenumbers (2 pi-periodized) for spectral derivatives
kx = 2*pi*fftfreq(Nx, d=dx)  # shape (Nx,)
ky = 2*pi*fftfreq(Ny, d=dy)  # shape (Ny,)
KX, KY = meshgrid(kx, ky, indexing="ij")
K2 = KX**2 + KY**2
L_op = M * K2                # Laplacian prefactor in CH

# Initial condition
phi = phi0_mean + eps * random_uniform(-1, 1, size=(Nx, Ny))

# Time stepping: semi-implicit (Eyre-type) split
# Treat - Laplacian(phi) implicitly, and the nonlinear f'(phi) explicitly.
# In Fourier space, the update for phi_hat is:
#   phi_hat^{n+1} = [phi_hat^n - dt * L_op * FFT( f'(phi^n) )]
#                    / [ 1 + dt * L_op * K2 ]

t = 0.0
while t < Tend:
    mu_prime = -phi + (phi**3)           # f'(phi)
    rhs_hat = FFT(phi) - dt * L_op * FFT(mu_prime)
    denom  = 1.0 + dt * L_op * K2
    phi = IFFT( rhs_hat / denom ).real
    t += dt

# Diagnostics:
# - Check mass conservation: mean(phi) ~ const.
# - Compute structure factor S(k) = <|phi_hat|^2>.
# - Track k_peak(t) where S(k) is maximal to analyze coarsening.
```

Lastly, we should provide the perspective that Cahn-Hilliard and models like it have found common use in the fields of Soft and Active Matter. This formalism can be coupled to reaction-diffusion type equations to model the growth and splitting of droplets [42], thereby addressing questions regarding the origin of life. Additionally, non-reciprocal interactions between two species that comprise a separating binary mixture have been considered [27]. This leads to intriguing travelling patterns, which may give insight into self-organized behavior in organisms. There is therefore much to explore beyond these lecture notes.

[1] J. Kim, S. Lee, Y. Choi, S.-M. Lee, and D. Jeong, *Basic principles and practical applications of the Cahn–Hilliard equation*, Math. Probl. Eng. **2016**, (2016).

[2] S. Xu, H. Zhou, Z. Sun, and J. Xie, *Formation of an fcc phase through a bcc metastable state in crystallization of charged colloidal particles*, Phys. Rev. E **82**, 010401 (2010).

[3] W. Gispen and M. Dijkstra, *Kinetic Phase Diagram for Nucleation and Growth of Competing Crystal Polymorphs in Charged Colloids*, Phys. Rev. Lett. **129**, 098002 (2022).

[4] W. Gispen, G. Coli, R. van Damme, C. Royall, and M. Dijkstra, *Crystal Polymorph Selection Mechanism of Hard Spheres Hidden in the Fluid*, ACS Nano **17**, 8807 (2023).

[5] B. Liu, T. Besseling, M. Hermes, A. Demirörs, A. Imhof, and A. Van Blaaderen, *Switching plastic crystals of colloidal rods with electric fields*, Nat. Commun. **5**, 3092 (2014).

[6] T. Welling, A. Grau-Carbonell, K. Watanabe, D. Nagao, J. de Graaf, M. van Huis, and A. van Blaaderen, *Frequency-controlled electrophoretic mobility of a particle within a porous, hollow shell*, J. Col. Interface Sci. **627**, 761 (2022).

[7] M. Zwolak and M. Di Ventra, *Colloquium: Physical approaches to DNA sequencing and detection*, Rev. Mod. Phys. **80**, 141 (2008).

[8] G. Rempfer, S. Ehrhardt, C. Holm, and J. de Graaf, *Nanoparticle translocation through conical nanopores: a finite element study of electrokinetic transport*, Macromolec. Theory Simul. **26**, 1600051 (2017).

[9] Y.-L. Ying *et al.*, *Nanopore-based technologies beyond DNA sequencing*, Nat. Nanotech. **17**, 1136 (2022).

[10] M. Mohammadi and O. Bavi, *DNA sequencing: an overview of solid-state and biological nanopore-based methods*, Biophys. Rev. **14**, 99 (2022).

[11] A. Van Blaaderen, J. Van Geest, and A. Vrij, *Monodisperse colloidal silica spheres from tetraalkoxysilanes: particle formation and growth mechanism*, J. Col. Interface Sci. **154**, 481 (1992).

[12] U. Gasser, E. Weeks, A. Schofield, P. Pusey, and D. Weitz, *Real-space imaging of nucleation and growth in colloidal crystallization*, Science **292**, 258 (2001).

[13] L. Filion, M. Hermes, R. Ni, and M. Dijkstra, *Crystal nucleation of hard spheres using molecular dynamics, umbrella sampling, and forward flux sampling: A comparison of simulation techniques*, J. Chem. Phys. **133**, 244115 (2010).

[14] W. Poon and M. Haw, *Mesoscopic structure formation in colloidal aggregation and gelation*, Adv. Col. Interface Sci. **73**, 71 (1997).

[15] E. Zaccarelli, *Colloidal gels: equilibrium and non-equilibrium routes*, J. Phys. Cond. Matt. **19**, 323101 (2007).

[16] J. de Graaf, W. Poon, M. Haughey, and M. Hermes, *Hydrodynamics strongly affect the dynamics of colloidal gelation but not gel structure*, Soft Matter **15**, 10 (2019).

[17] R. Larson, *The structure and rheology of complex fluids* (Oxford University Press (New York), ADDRESS, 1999), Vol. 150.

[18] R. Mezzenga, P. Schurtenberger, A. Burbidge, and M. Michel, *Understanding foods as soft materials*, Nat. Mater. **4**, 729 (2005).

[19] M. Faers, T. Choudhury, B. Lau, K. McAllister, and P. Luckham, *Syneresis and rheology of weak colloidal particle gels*, Col. Surf. A. Physicochem. Eng. Asp. **288**, 170 (2006).

[20] A. Darras, A. Dasanna, T. John, G. Gompper, L. Kaestner, D. Fedosov, and C. Wagner, *Erythrocyte sedimentation: Collapse of a high-volume-fraction soft-particle gel*, Phys. Rev. Lett. **128**, 088101 (2022).

[21] J. Cahn and J. Hilliard, *Free energy of a nonuniform system. I. Interfacial free energy*, J. Chem. Phys. **28**, 258 (1958).

[22] J. Verhoeven, A. Pendray, and E. Gibson, *Wootz Damascus steel blades*, Mater. Character. **37**, 9 (1996).

[23] R. Choksi, M. Peletier, and J. Williams, *On the phase diagram for microphase separation of diblock copolymers: an approach via a nonlocal Cahn–Hilliard functional*, SIAM J. Appl. Math. **69**, 1712 (2009).

[24] A. Agosti, P. Antonietti, P. Ciarletta, M. Grasselli, and M. Verani, *A Cahn-Hilliard–type equation with application to tumor growth dynamics*, Math. Methods Appl. Sci. **40**, 7598 (2017).

[25] P. Seppecher, *Moving contact lines in the Cahn-Hilliard theory*, Int. J. Eng. Sci. **34**, 977 (1996).

[26] Q.-X. Liu, A. Doelman, V. Rottschäfer, M. de Jager, P. Herman, M. Rietkerk, and J. van de Koppel, *Phase separation explains a new class of self-organized spatial patterns in ecological systems*, Proc. Nat. Acad. Sci. **110**, 11905 (2013).

[27] S. Saha, J. Agudo-Canalejo, and R. Golestanian, *Scalar active mixtures: the nonreciprocal Cahn-Hilliard model*, Phys. Rev. X **10**, 041009 (2020).

[28] A. Archer, D. Ratliff, A. Rucklidge, and P. Subramanian, *Deriving phase field crystal theory from dynamical density functional theory: consequences of the approximations*, Phys. Rev. E **100**, 022140 (2019).

[29] M. Te Vrugt and R. Wittkowski, *Perspective: New directions in dynamical density functional theory*, J. Phys. Cond. Mat. **35**, 041501 (2022).

[30] M. te Vrugt, H. Löwen, and R. Wittkowski, *Classical dynamical density functional theory: from fundamentals to applications*, Adv. Phys. **69**, 121 (2020).

[31] D. Lee, J.-Y. Huh, D. Jeong, J. Shin, A. Yun, and J. Kim, *Physical, mathematical, and numerical derivations of the Cahn–Hilliard equation*, Comput. Mater. Sci. **81**, 216 (2014).

[32] W. Boettinger, J. Warren, C. Beckermann, and A. Karma, *Phase-field simulation of solidification*, Ann. Rev. Mater. Research **32**, 163 (2002).

[33] A. Miranville, *The Cahn–Hilliard equation and some of its variants*, AIMS Math. **2**, 479 (2017).

[34] A. Archer and R. Evans, *Dynamical density functional theory and its application to spinodal decomposition*, J. Chem. Phys. **121**, 4246 (2004).

[35] S. van Teeffelen, R. Backofen, A. Voigt, and H. Löwen, *Derivation of the phase-field-crystal model for colloidal solidification*, Phys. Rev. E **79**, 051404 (2009).

[36] G. Wilemski, *On the derivation of Smoluchowski equations with corrections in the classical theory of Brownian motion*, J. Stat. Phys. **14**, 153 (1976).

[37] H. Risken and T. Caugheyz, *The Fokker-Planck Equation: Methods of solution and application* (Springer, New York (USA), 1991).

[38] J. Brady and G. Bossis, *Stokesian Dynamics*, Ann. Rev. Fluid Mech. **20**, 111 (1988).

[39] R. Wittkowski, A. Tiribocchi, J. Stenhammar, R. Allen, D. Marenduzzo, and M. Cates, *Scalar φ^4 field theory for active-particle phase separation*, Nat. Commun. **5**, 4351 (2014).

[40] H. Garcke, B. Niethammer, M. Rumpf, and U. Weikard, *Transient coarsening behaviour in the Cahn–Hilliard model*, Act. Mater. **51**, 2823 (2003).

[41] B. König, O. Ronsin, and J. Harting, *Two-dimensional Cahn–Hilliard simulations for coarsening kinetics of spinodal decomposition in binary mixtures*, Phys. Chem. Chem. Phys. **23**, 24823 (2021).

[42] D. Zwicker, R. Seyboldt, C. Weber, A. Hyman, and F. Jülicher, *Growth and division of active droplets provides a model for protocells*, Nat. Phys. **13**, 408 (2017).